Gated-region transport in the quantum Hall effect

J. M. Ryan, N. F. Deutscher, and D. K. Ferry
Center for Solid State Electronics Research, Arizona State University, Tempe, Arizona 85282-6202
(Received 18 March 1993)

We study the quantum Hall effect in samples in which a portion of the longitudinal conduction path is gated. Full magnetic-field sweeps were taken on a sample consisting of a gated Hall bar geometry. These data yielded plateaus in longitudinal resistance, as the gate voltage is varied, for the integer filling factor in the bulk, as previously observed, and plateaus for the case of a fixed integer number of transmitted edge states under the barrier as the gate voltage and the magnetic field are varied. For a significant portion of the Shubnikov–de Haas sweeps, the barrier region dominates the characteristic conductance and Fourier analysis allows one to determine the variation of the carrier concentration in the gated region as a function of gate voltage.

INTRODUCTION

The study of the quantum Hall effect, in which the Hall resistance is quantized exactly in units of h/e^2, has focused over the last few years upon the role played by edge states in transport through the overall device.[1] These edge states are thought to provide essentially dissipation-free transport from a current-injecting contact to the current-sinking contact, so that the quantized Hall conductance can be computed from the Büttiker-Landauer formula[2] in terms of transmission coefficients through the structure. The role of these edge states has previously been examined in gated structures, and it has been shown that a gate selectively reflects a fraction of the occupied edge states.[3,4] Both Büttiker[5] and van Houten and co-workers[6] have shown that when a quantum Hall bar is biased with a perpendicular magnetic field, such that the filling factor away from the gate is an integer N, a gate barrier which reflects K edge states leads to a quantized longitudinal resistance in accordance with

$$R_{\text{longitudinal}} = \frac{h}{e^2}\frac{K}{N(N-K)} . \tag{1}$$

This equation can be rewritten in the original form of Büttiker as[5]

$$R_{\text{longitudinal}} = \frac{h}{e^2}\left[\frac{1}{N'}-\frac{1}{N}\right] , \tag{2}$$

where $N'=N-K$ is the number of edge states transmitted through the barrier.

It has been shown that by fixing N (constant magnetic field), increasing the barrier height results in quantized values of the longitudinal resistance in accordance with (1) and (2) for barriers able to completely reflect an edge channel.[3,4] In contrast, we have previously shown that for samples biased with barriers created from ultrasubmicron gates ($L_g=50$ nm), the plateaus predicted from (1) and (2) are not formed, due to the presence of significant tunneling of the incident edge channels through the depletion region.[7]

In this study we have set out to study more extensively the role of the barrier throughout the entire magnetic-field range. By biasing the bulk of the sample to noninteger filling factors, and then varying the barrier height, we can probe directly the edge states under the barrier, as well as in the ungated bulk. In this method, it can be seen that the transport varies from two-dimensional to one-dimensional under the barrier, as the filling factor of this region is varied, and back to two-dimensional again. Similar behavior is experienced as one moves away from the barrier as the current traverses the region. The case of a constant N' (edge states under the barrier are fixed to an integer number independent of the barrier height) is investigated and quantized values of the longitudinal resistance are observed in accordance with (2). These are compared to the case of constant N (edge states away from the barrier are fixed to an integer number independent of barrier height). Additionally, by use of a Fourier transform to determine the frequency of the Shubnikov–de Haas oscillations in the longitudinal resistance, as the barrier height is increased, the dominant factor in edge-state transport is shown to be the barrier region and not the much larger undisturbed edge-state region away from the barrier.

SAMPLE PREPARATION

The devices were fabricated from GaAs/$Al_xGa_{1-x}As$ heterojunction material, with a nominal two-dimensional density of 4×10^{11} cm^{-2} and a mobility of 4×10^5 cm^{2}V s, both at 1.4 K. The layers consisted of molecular-beam-epitaxy growth 1-μm undoped GaAs buffer, a 20-nm undoped $Ga_xAl_{1-x}As$ ($x=0.3$) spacer layer, a 30-nm 1×10^{18} Si-doped $Ga_xAl_{1-x}As$ ($x=0.3$) layer, and a 5-nm undoped GaAs cap layer. The device was patterned into a Hall bar with six side arms and a 20-μm gate was placed across the longitudinal axis between adjacent side arms, so that the longitudinal conductance could be simultaneously measured in both the gated and ungated regions, in order to isolate the effects of the gate. The Hall bar geometry was defined by wet etching. The Ohmic contacts were AuGeNi alloyed at 450 °C for 40 sec by

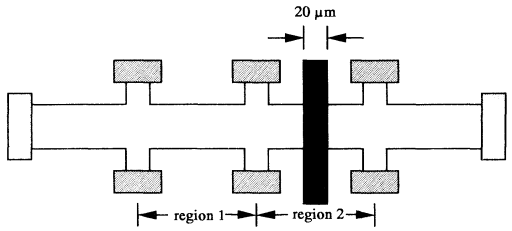

FIG. 1. Schematic representation of the device. A 20-μm gate is situated between adjacent side arms in region 2 to allow longitudinal transport to be compared by simultaneous measurements of ungated (region 1) and gated (region 2) portions of the sample. This allows us to isolate the effects of the gate. The width of the longitudinal part of the sample is 30 μm, and the 20-μm-wide side arms are spaced by 90 μm (center to center).

rapid thermal annealing (RTA). The gate itself was a nonrecessed, 100-nm-thick Au layer. The Ohmic contacts and the gate were connected to 300×300 μm^2 bonding pads to allow connection for mounting to the ceramic flat package. A schematic of the active area of the device is shown in Fig. 1. The measurements were performed using a lock-in technique with a current bias of 10 nA at 1.4 K, in a Janis He^4 superconducting magnet, and with magnetic fields up to 9 T.

RESULTS

Depending on the recent history of the device, it would act as either a depletion- or accumulation-mode device. For the results presented here, the device was operated in the accumulation mode with a "decoupling" bias of 0.65 V needed to equate the density in regions 1 and 2 (Fig. 1). To determine the decoupling bias needed for the gate, the gate voltage is first varied until the density is roughly equal in region 1 (ungated) and region 2 (gated), as inferred from the two-dimensional sheet density obtained from the Shubnikov–de Haas oscillations. As will be shown later, it was not possible to fully equate these densities, as region 2 would always retain a slightly lower density. Once the decoupling voltage is determined and applied to the gate, the channel is considered to be fully open. The Hall and longitudinal resistances for regions 1 and 2 are shown in Fig. 2 with a positive voltage of 0.66 V applied to the gate.

A series of magnetic-field sweeps, at different gate voltages, was performed over the range 0–9 T, with gate voltage steps of 10 mV. Varying the magnetic field allowed the entire spectrum of filling factors in both the gated and the ungated regions to be examined. As expected, the longitudinal sweeps of region 1 are completely unaffected by sweeping the gate bias in region 2, since the edge channels are re-equilibrated by the side arm.[8] A series of sweeps for region 2 is shown in Fig. 3. By taking a cross-sectional slice through the data at a fixed magnetic field, corresponding to a constant filling factor in region 1, the constant N case of edge-state gating is recovered. This is shown in Fig. 4, with the individual curves offset by 10 kΩ for clarity. The expected plateaus, from (1), are indicated by the arrows and labeled with the corresponding N' values. As may be seen in Fig. 4, the plateaus are observed in agreement with previous studies[3,4] and with (1). We note that this method allows one to probe the spin-split minima as well as those for completely full Landau levels in the ungated part of the sample.

In Fig. 3, it appears that the minima for the $N=2,3,4,6,\ldots$ filling factors appear to shift to a lower magnetic field as the gate depletion is increased, suggesting a reduction in density. This is, in fact, expected to occur under the gate. However, it suggests that the overall longitudinal conductance is dominated by the resistive contributions of the gated region. This will allow us to examine the density by looking at the Fourier transforms of these traces. Since the behavior should be periodic in $1/B$, the Fourier transform needs to be taken in $1/B$. Experimentally we are limited to taking data at regular intervals of B rather than $1/B$. It is possible to reconstruct a bandlimited signal from nonuniform samples t_n if there exists a bijective function $\gamma(t_n)$ that maps the nonuniform samples into uniform samples[9]

$$\gamma(t_n)=nT \ . \tag{3}$$

If the function $h(t)$ is the nonuniformly sampled signal,

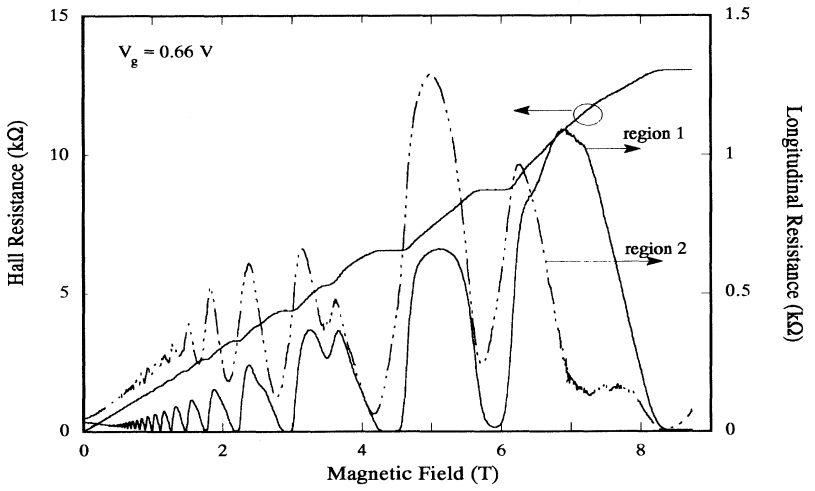

FIG. 2. The measured Hall and longitudinal resistances for the gated (region 2) and ungated (region 1) portions of the samples at 1.4 K with a fully "undepleted" gate voltage applied to the gate (+0.66 V). Also shown is the Hall resistance.

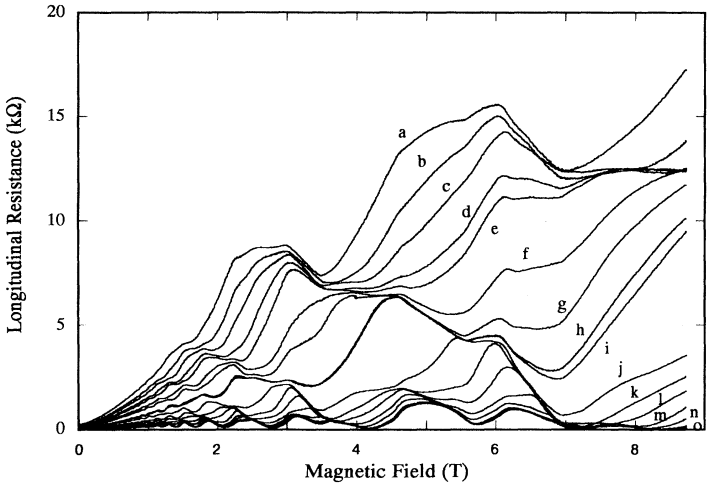

FIG. 3. The longitudinal resistances for region 2 for a variety of gate voltages. Sweeps $a-o$ are for +0.12, 0.15, 0.18, 0.21, 0.24, 0.27, 0.3, 0.33, 0.36, 0.42, 0.45, 0.48, 0.51, 0.54, and 0.57 V applied to the gate, respectively.

and $f(\tau)$ a uniformly sampled signal equal to $h(t)$, they are related by

$$h(t)=f\{\gamma(t)\}=f(\tau)\ ,$$
$$h(t_n)=f\{\gamma(t_n)\}=f(nT)\ . \tag{4}$$

The signal $h(t)$ can be reconstructed from the sampling theorem,

$$h(t)=f(\tau)=\sum\frac{f(nT)\sin\{\omega_0(\tau-nT)\}}{\omega_0(\tau-nT)}$$
$$=\sum\frac{h(t_n)\sin\{\omega_0[\gamma(t)-nT]\}}{\omega_0(\gamma(t)-nT)}\ . \tag{5}$$

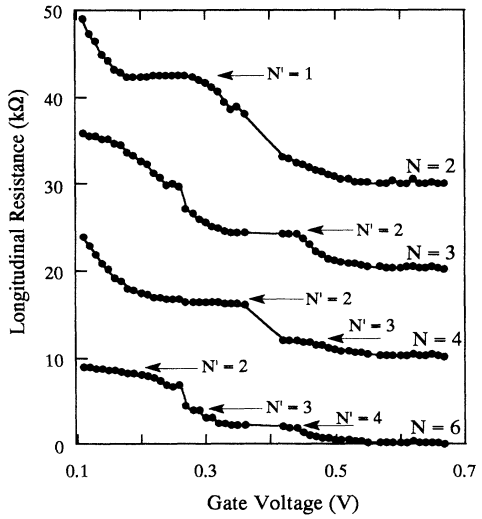

FIG. 4. The longitudinal resistance at fixed magnetic field values of 8.5, 5.85, 4.4, and 2.9 T, corresponding to integer filling factors (in the ungated region) of 2, 3, 4, and 6, respectively, obtained from the magnetic-field sweeps shown in Fig. 3. The expected positions of various plateaus are identified by the arrows and the filling factor in the gated region. The curves are offset by 10 k Ω for clarity.

For the situation we are concerned with, the mapping function is simply

$$\gamma(t)=\frac{1}{t} \tag{6}$$

and a discrete transform can be found from the uniformly sampled signal

$$F_m=\frac{1}{N}\sum_{n=0}^{N-1}f(nT)e^{-i2\pi mn/N},\quad m=0,1,\ldots,N-1\ . \tag{7}$$

Before the Fourier transform is taken, a Parzen window is applied to reduce spectral power leakage from one "bin" into neighboring "bins," and has the form

$$\omega_j=1-\left|\frac{j-\frac{1}{2}(N-1)}{\frac{1}{2}(N+1)}\right|\ . \tag{8}$$

In Fig. 5, two Shubnikov–de Haas traces are shown, one for region 1 (ungated) and one for region 2 (gated). The sweep for the gated region has a positive bias of 0.45 V applied to the gate, so that it is somewhat depleted with respect to the ungated region. The Fourier transforms (in $1/B$) are shown in Fig. 6. The corresponding Fourier transform for the sweep with a gate bias of 0.66 V, taken from Fig. 2, is also shown in Fig. 6. As can be seen from this latter figure, region 1 clearly shows a single strong peak near 8.75 T, labeled peak 1, which corresponds to the first subharmonic, and the fundamental peak at 17.5 T. Because the spin-split filling factors are not well developed, compared to the even filling factors, and we do not reach a magnetic field corresponding to $N=1$, the fundamental frequency is significantly weaker than the first subharmonic. It is this first subharmonic that we will concentrate on in the remainder of the paper. These two peaks correspond to a density of 4.22×10^{11} cm^{-2}, which is in agreement with the inferred density previously obtained from the Hall constant.

The gated region also shows a peak essentially at the same position as the ungated region of the sample, and is therefore labeled peak 1. The position of this peak does not shift as a function of applied gate voltage. We therefore assume that this peak arises from the contributions

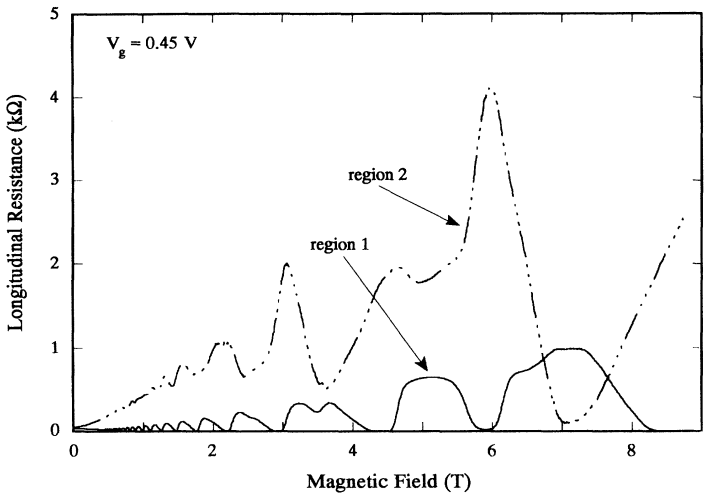

FIG. 5. The measured longitudinal resistances for region 1 (ungated) and region 2 (gated) with a voltage of +0.45 V applied to the gate. Here, it is clear that the density in the gated region is considerably lower than that in the ungated region, and this is evident in the Shubnikov–de Haas behavior.

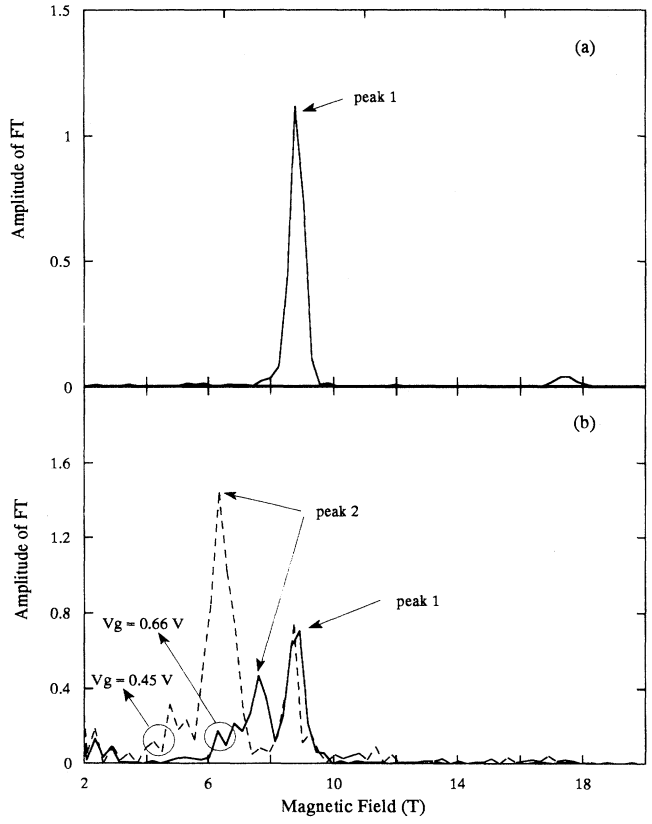

FIG. 6. (a) The Fourier transform (reciprocal magnetic field) of the longitudinal resistance of region 1 (ungated). Peak 1 is the first subharmonic of the fundamental period (shown near 17.5 T), and is much stronger due to the lack of the $N=1$ plateau in the data series. (b) The equivalent Fourier transforms for region 2 (gated) sweeps at two different values of the gate voltage (+0.66 and +0.45 V). While peak 1 remains relatively unchanged, the position and amplitude of peak 2 varies with the gate voltage.

to the overall resistance from those portions of region 2, which are not under the barrier. As can be observed, a second peak, labeled peak 2, is also present in the gated region sweeps, even with the decoupled voltage applied to the gate. This peak is due to the resistance contributions from the reduced density region under the gate barrier itself. The amplitude of peak 2 increases in magnitude, and the peak itself shifts to lower frequency (implying a lower density), as the barrier height is increased. We plot the position of these two peaks in Fig. 7 as a function of the gate voltage. To reiterate, the data in Fig. 7, for both peaks, arise from a single Shubnikov–de Haas magnetic-field sweep measured across the two side arms of region 2 (Fig. 1). The error bars represent the spectral width of the transform that is introduced by the windowing of the data; e.g., the result of a finite range of magnetic field. Within experimental error, the position of peak 1 (in region 2) does not shift as a function of gate voltage. Peak 2, however, decreases roughly linearly as a function of voltage, as expected if the gate voltage linearly moves the Fermi energy in the degenerate two-dimensional electron gas. The density decreases by approximately a factor of 2 over the range of gate voltage shown. The straight line drawn through the points is merely to guide the eye (and is not a fit to the data); but it is evident that simply increasing the applied gate voltage does not completely eliminate the gate from transport measurements. Since the gates were not recessed, it would seem probable that applying sufficient positive voltage could lead to a higher density under the gate than in the ungated bulk region; but this is not the case, at least in these samples.

The ratio of the amplitude of the two peaks is plotted as a function of gate voltage in Fig. 8. From this figure, it is evident that, as the barrier is increased (applied gate voltage $\rightarrow$0 V), the dominant frequency primarily arises from the region of reduced density under the gate, and it is this region that determines the nature of the longitudinal transport through the device. From Fig. 8, the minimum around 0.58 V indicates that the role of the

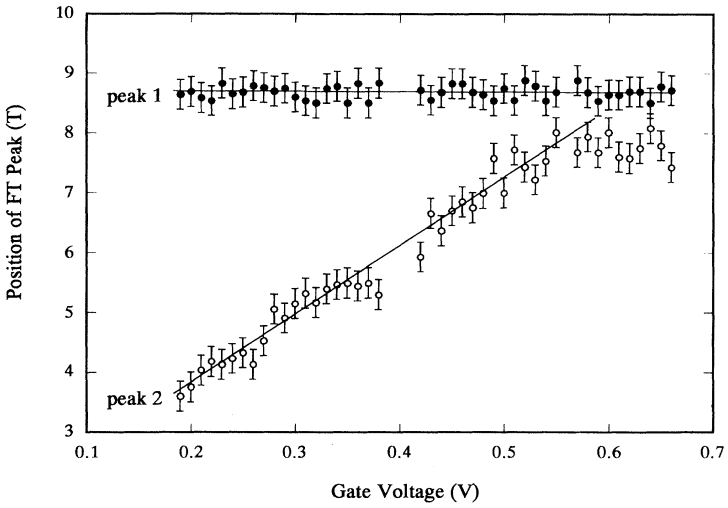

FIG. 7. The position of the two main peaks in the Fourier transforms of the gated-region longitudinal resistance, as a function of gate voltage. Peak 1 does not shift position, indicating that it arises from that portion of region 2 not directly under the gate-depletion region, while peak 2 shifts as a function of gate voltage as is expected from a peak arising from that portion actually in the depletion region.

barrier again increases in what would be expected to be the accumulation range, even though Fig. 7 indicates the density in this region of gate voltages is pinned to a level just under accumulation.

From the data contained in Fig. 7, the density of the region under the barrier can be determined as a function of both gate voltage and magnetic field, so that it is now possible to examine the case for a fixed number of edge states under the barrier, independent of barrier height (constant N'). This corresponds to following (2) along the lines indicated in Fig. 9. By fixing N' and varying N, plateaus are predicted from (2) whenever N reaches an integer value. That is, we pick a fixed value of N' and plot the longitudinal resistance as the gate voltage is varied, but using a magnetic-field value such that the filling factor under the gate remains constant. This is plotted in Fig. 10 for the $N'=2$, 4, and 6 cases and results in good agreement with the expected positions of the plateaus, although the plateaus here are not as well formed as for the case of constant N. For the constant N' traces, a limiting resistance value of $h/N'e^2$ will be approached as $N\rightarrow\infty$, in contrast to the infinite resistance in the constant N case as the barrier completely depletes the channel. The reason the N' traces do not approach their limiting values here is that the current, held constant as required for quantum Hall-effect measurements, is forced into the buffer layer thus destroying the two-dimensional nature of the sample as the barrier height is increased. To prevent this from occurring, the gate voltage was limited to values less than the full channel pinchoff. To follow a constant N' trace for an odd index was more difficult, since the spin-split levels are not resolved at low magnetic field. Figure 11 shows a constant $N'=3$ trace which forms a plateau at $N=4$, but there are only hints at formation of the $N=6$ and 8 plateaus before the edge state is no longer well resolved.

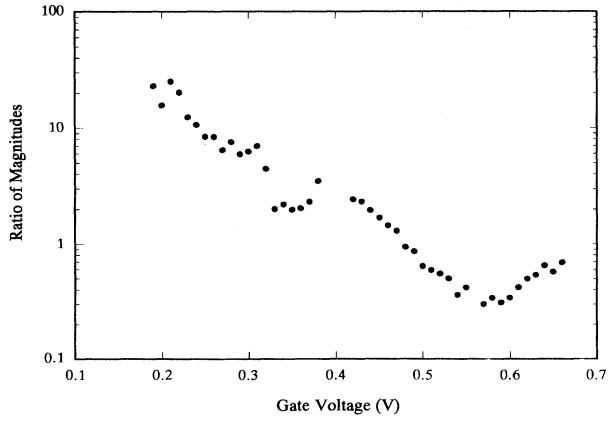

FIG. 8. The relative magnitude of the Fourier transform peak 2 to peak 1 as a function of gate voltage for the gated region. Here, the ratio is that of the intensities (the actual ratio of amplitudes plotted in Fig. 6 for example).

DISCUSSION

It is clear that the Shubnikov–de Haas measurements across a gated region show the effects of both the region under the gate and the parts of the sample outside of this region. When the bulk of the sample is near a Hall plateau, so that the longitudinal conductance is near zero, it is easy to understand why the resistance of the gate region dominates the entire region. On the other hand, when the region under the gate is near a Hall plateau, the ungated region dominates the overall resistance. Although is it not truly possible to say that these two resistance regions are connected in series for the ballistic-transport mode appropriate to the edge states,[2] it is apparent that the oscillatory properties of both regions appear in the overall resistance. As the resistance of the gated region becomes higher, with depletion of this region, this resistance plays a larger role in the overall properties, as exhibited in the growing strength of peak 2 in Fig. 8.

It is worth comparing the results obtained here with a diagonal measurement used to study the density under a gate, as reviewed by Beenakker and van Houten.[10] In this latter measurement, the Hall resistance and the lon-

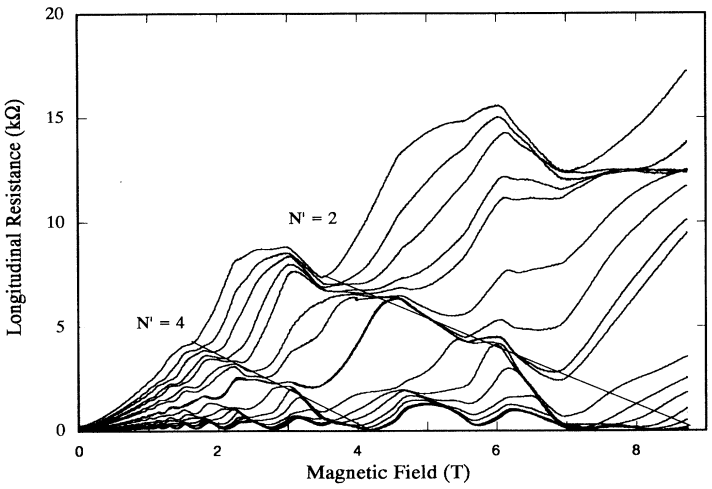

FIG. 9. Longitudinal resistance for the gated region as a function of magnetic field. The curves here are exactly those in Fig. 2. The lines are rough estimates of the position of minima resulting from a constant number N' of edge states under the barrier. The two shown are for $N'=2$ and 4.

gitudinal resistance are determined by a diagonal measurement which yields $R_H \pm R_L$ (the sign depends upon the orientation of the measurements, and shown in Fig. 82 of Ref. 10). When the number of edge states in both the gated and ungated regions are integers, the density can be inferred from the use of (2), and an equivalent equation for the Hall resistance on the plateau. However, when these quantities are not both integers, this approach can lead to errors. Consider, for example, Fig. 3 in the region around $B=8.5$ T. Here, $N=2$ in the ungated region. If we look at curve h, which is for $V_G=0.33$ V, the longitudinal resistance varys quite rapidly as a function of the magnetic field across the plateau. However, the density in the gated region is not changed significantly, and may be inferred to be approximately 2.5×10^{11} cm^{-2} from Fig. 7. The longitudinal resistance is composed of two competing Shubnikov–de Haas series, due to the two regions (gated and ungated), and only near a plateau can the diagonal method be used with confidence.

As can be seen from Fig. 3, not all of the observable structures in the Shubnikov–de Haas spectra can be accounted for by the above discussions. Most obvious is the structure observed between the $N=2$ and 3 minima in Fig. 2. There is an indication of a minimum at approximately 7 T in the curve for the ungated region. The po-

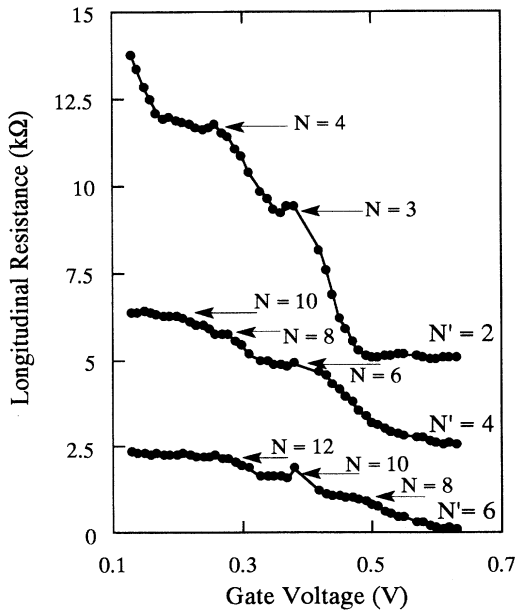

FIG. 10. The longitudinal resistance for a fixed (even) number N' of edge states under the barrier. The positions of the expected plateaus are indicated by the arrows. The curves are offset by 2.5 kΩ for clarity.

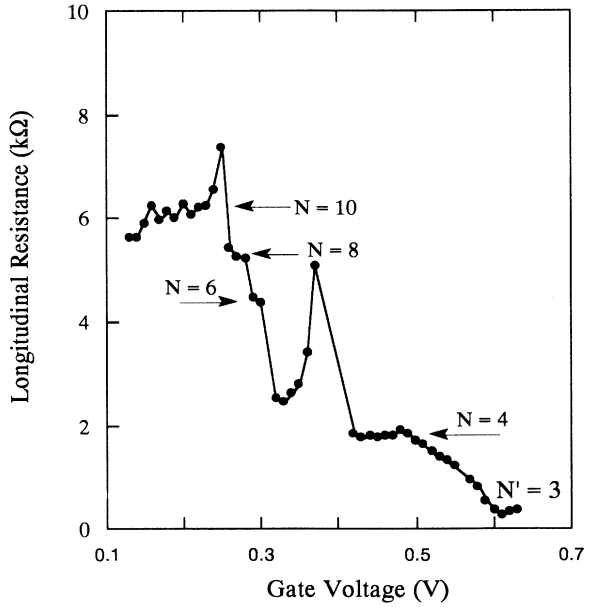

FIG. 11. The longitudinal resistance for a fixed $N'=3$ under the barrier, as a function of gate voltage. The position of the expected plateau is indicated by the arrows. It is clear that there is a variety of saddle-point and non-saddle-point tunneling transitions in the curves, where these quantities are defined in the terminology of Ref. 3.

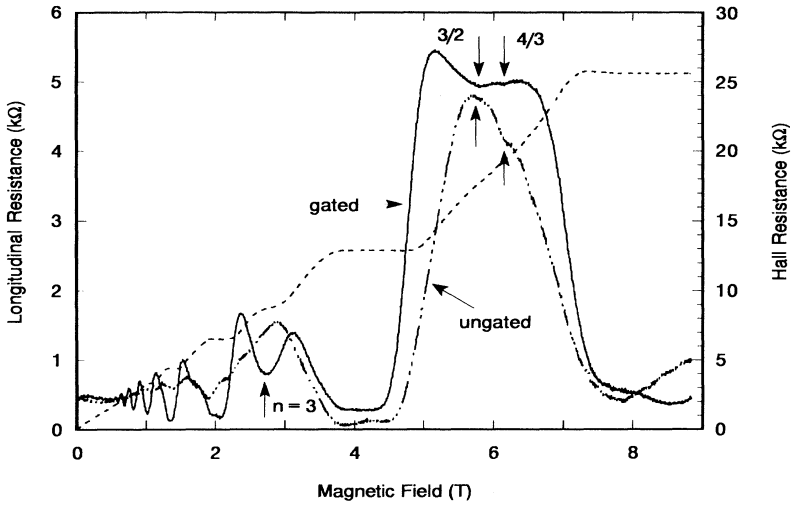

FIG. 12. The longitudinal and Hall resistance for a device with three small gates (50-nm gates on 200-nm pitch) illustrating the enhancement and formation of certain fractional filling factors. This device was prepared from the same material as the devices discussed previously.

sition of this point seems to be appropriate to the $\frac{7}{3}$ fractional level, but this is usually not well formed at 1.4 K, where these measurements are made. However, this minimum is enhanced and forms the much flatter region observed in the curve for the gated region 2. This structure does not shift in position as a function of barrier height, indicating it is in that portion of region 2 not under gate metallization. Nevertheless, its behavior is enhanced by the presence of the gate. We do not understand how a fractional state could be enhanced by the presence of the gate, unless there is significant nonequilibrium population of the edge states involved,[11] due to the potentials in the vicinity of the gate.[12] We also note that there is some indication of a $\frac{4}{3}$ (5.5 T) and $\frac{7}{3}$ (2.8 T) dip in the longitudinal conductance at the highest level of depletion (upper curve) shown in Figs. 2 and 9, and these are shifted in density as the region under the gate is depleted. The existence of fractional edge states in depletion-gated devices has been used to explain other results, although at much lower temperatures,[12,13] and it is possible that the presence of these states contributes to the tunneling process. On a device fabricated from the same material but with a gate structure consisting of three 50-nm gates on a 200-nm period, and operating in the depletion mode, a similar enhancement was also observed. It is shown in Fig. 12. The enhanced fraction for this gated structure is centered around a magnetic-field value suggesting a $\frac{3}{2}$ or a combination of odd denominators merging together to form a fractional edge state along the barrier. This structure was only present in the gated region of the sample. We remark, however, that an alternative interpretation of these extra "minima" could be in terms of just effects arising from poor contacts.[10,14,15] Contacts which do not interact equally with all edge states are known to lead to strange behavior, quite similar to that observed here, which is interpreted in terms of anomalous suppression of some of the Shubnikov–de Haas oscillations. While it is not possible to delineate whether these are real minima, or are just contact effects, it is strange that the effects described here would arise from contact effects that occur only at very specific values of the magnetic field and often remain even after other expected minima are destroyed by gating.

ACKNOWLEDGMENTS

This work was supported by the office of Naval Research. The authors would like to express their appreciation to Y. Takagaki, M. A. Reed, F. Kuchar, and K. Connolly for many helpful discussions. The authors also want to express their appreciation to E. Paris, Thomson-CSF, for furnishing the material used.

[1]See, e.g., D. B. Chklovskii, B. I. Shklovskii, and L. I. Glazman, Phys. Rev. B **46**, 4026 (1992), and references contained therein.

[2]M. Büttiker, Y. Imry, R. Landauer, and S. Pinhas, Phys. Rev. B **31**, 6207 (1985).

[3]R. J. Haug, A. H. MacDonald, P. Streda, and K. von Klitzing, Phys. Rev. Lett. **61**, 2797 (1988); R. J. Haug, J. Kucera, P. Streda, and K. von Klitzing, Phys. Rev. B **39**, 10 892 (1989).

[4]S. Washburn, A. B. Fowler, H. Schmid, and D. Kern, Phys. Rev. Lett. **61**, 2801 (1988).

[5]M. Büttiker, Phys. Rev. B **38**, 9375 (1988); in *Nanostructure Physics and Fabrication,* edited by M. A. Reed and W. P. Kirk (Academic, New York, 1989), p. 319.

[6]C. W. J. Beenakker and H. van Houten, Phys. Rev. Lett. **60**, 2406 (1988); H. van Houten, C. Beenakker, P. van Lossdrecht, T. Thornton, H. Ahmed, M. Pepper, C. Foxon, and J. Harris, Phys. Rev. B **37**, 8534 (1988).

[7]J. M. Ryan, N. F. Deutscher, and D. K. Ferry, Phys. Rev. B **47**, 16 594 (1993).

[8]G. Müller, D. Weiss, S. Koch, and K. von Klitzing, Phys. Rev. B **42**, 7633 (1990).

[9]J. J. Clark, M. R. Palmer, and P. D. Lawrence, IEEE Trans. Acoust. Speech, Signal Process. **33**, 1151 (1985).

[10]C. W. J. Beenakker and H. van Houten, in *Solid State Physics: Advances in Research and Applications,* edited by H. Ehrenreich and D. Turnbull (Academic, New York, 1991), Vol. 44,

p. 1.
[11]L. P. Kouwenhoven, B. J. van Wees, N. C. van der Vaart, C. J. P. M. Harmans, C. E. Timmering, and C. T. Foxon, Phys. Rev. Lett. **64**, 685 (1990); A. M. Chang and L. E. Cunningham, *ibid.* **69**, 1992.
[12]A. H. MacDonald, Phys. Rev. Lett. **64**, 220 (1990).
[13]C. W. J. Beenakker, Phys. Rev. Lett. **64**, 216 (1990).
[14]B. J. van Wees, E. M. M. Williams, L. P. Kouwenhoven, C. J. P. M. Harmans, J. G. Williamson, C. T. Foxon, and J. J. Harris, Phys. Rev. B **39**, 8066 (1989).
[15]S. Komiyama, H. Hirai, M. Ohsawa, Y. Matasuda, S. Sasa, and T. Fuji, Phys. Rev. B **45**, 11 085 (1992).